

OSCAR: Orchestrated Self-verification and Cross-path Refinement

Yash Shah*

Arizona State University
yshah124@asu.edu

Abhijit Chakraborty*

Arizona State University
achakr40@asu.edu

Naresh Kumar Devulapally

University at Buffalo, SUNY
devulapa@buffalo.edu

Vishnu Lokhande

University at Buffalo, SUNY
vishnulo@buffalo.edu

Vivek Gupta

Arizona State University
vgupt140@asu.edu

Abstract

Diffusion language models (DLMs) expose their denoising trajectories, offering a natural handle for inference-time control; accordingly, an ideal hallucination mitigation framework should intervene during generation using this model-native signal rather than relying on an externally trained hallucination classifier. Toward this, we formulate *commitment uncertainty localization*: given a denoising trajectory, identify token positions whose cross-chain entropy exceeds an unsupervised threshold before factually unreliable commitments propagate into self-consistent but incorrect outputs. We introduce a suite of trajectory-level assessments, including a cross-chain divergence-at-hallucination (CDH) metric, for principled comparison of localization methods. We also introduce OSCAR, a training-free inference-time framework operationalizing this formulation. OSCAR runs N parallel denoising chains with randomized reveal orders, computes cross-chain Shannon entropy to detect high-uncertainty positions, and then performs targeted remasking conditioned on retrieved evidence. Ablations confirm that localization and correction contribute complementary gains, robust across $N \in \{4, 8, 16\}$. On TriviaQA, HotpotQA, RAGTruth, and CommonsenseQA using LLaDA-8B and Dream-7B, OSCAR enhances generation quality by significantly reducing hallucinated content and improving factual accuracy through uncertainty-guided remasking, which also facilitates more effective integration of retrieved evidence. Its native entropy-based uncertainty signal surpasses that of specialized trained detectors, highlighting an inherent capacity of diffusion language models to identify factual uncertainty that is not present in the sequential token commitment structure of autoregressive models. We are releasing the codebase¹ to support future research on localization and uncertainty-aware generation in DLMs.

1 Introduction

The Transformer architecture (Vaswani et al., 2017) revolutionized sequence modeling by replacing recurrence with self-attention, leading to autoregressive (AR) decoding for token generation. This enables hallucination detection tools like perplexity thresholding and retrieval-augmented verification (Farquhar et al., 2024; Malinin & Gales, 2021; Lewis et al., 2020; Tonmoy et al., 2024). Diffusion language models (DLMs) generate text through iterative demasking from masked sequences (Nie et al., 2025; Ye et al., 2025). Unlike autoregressive LLMs, DLMs maintain a trajectory (Li et al., 2025) of intermediate states encoding uncertainty, impacting question answering where early errors cause hallucination crystallization (Lu et al., 2024). These research threads hallucination detection in language models

*Equal contribution.

¹<https://anonymous.4open.science/r/dllm-hallucination-332B/README.md>

and denoising dynamics of diffusion models developed largely in parallel. Detection literature focuses on classifiers recognizing hallucinations post-generation, while DLM literature characterizes trajectory-level phenomena without exploiting them for correction. These threads converge: DLM denoising’s order-dependence of token commitment directly yields an uncertainty signal that detection literature trains classifiers to approximate (Bloem-Reddy & Teh, 2020). OSCAR bridges this gap by transforming a diagnostic signal into a correction mechanism.

Prior work on hallucination detection includes *output-based* methods (Kuhn et al., 2023; Lin et al., 2024; Ren et al., 2023; Malinin & Gales, 2021) analyzing final output, *latent-based* methods (Burns et al., 2024; Park et al., 2025; Azaria & Mitchell, 2023; Chen et al., 2024) probing internal representations, and *trajectory-based* methods TraceDet (Chang et al., 2025), DynHD (Qian et al., 2026) exploiting multi-step dynamics. Trajectory-based methods achieve strongest results but require trained classifiers that may not transfer across domains. These methods only flag hallucinations without correction. This is due to AR-based tools’ incompatibility with bidirectional denoising, lack of ground-truth signals, and underutilized trajectory data. (Niu et al., 2024; Min et al., 2023; Tonmoy et al., 2024).

We argue that rather than training classifiers to recognize hallucinations after generation, we should exploit the *native uncertainty signal* from DLMs. Our key observation is:

If multiple denoising chains, each following a different randomized reveal order, disagree on a token position, that position is factually uncertain; regardless of how confident any single chain appears.

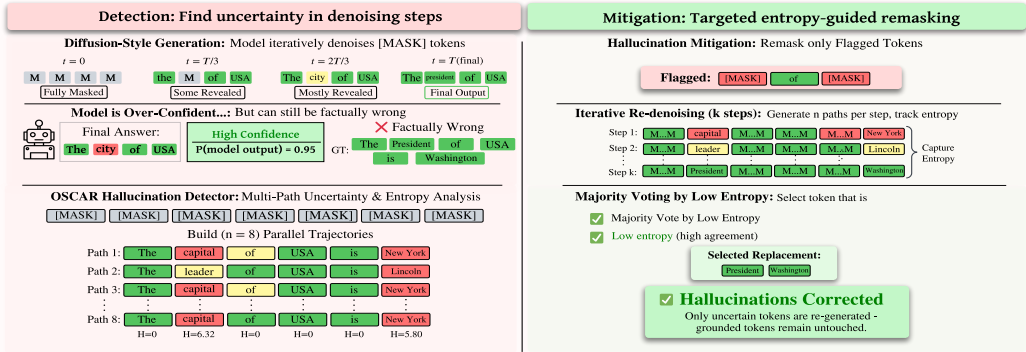


Figure 1: Schematic overview of the OSCAR pipeline, illustrating the key stages and components involved in the process.

This leads to **commitment uncertainty localization** (§3): given parallel denoising trajectories, identify token positions where cross-chain Shannon entropy exceeds an unsupervised threshold, *before* premature commitments lead to incorrect outputs. The **Adaptive Re-marking and Re-denoising Phase** (§3) then selectively remarking uncertain token spans and re-denoises them, enabling targeted correction based on uncertainty signal. We implement these in OSCAR (**O**rchestrated **S**elective **C**orrection via **A**daptive **R**emarking), a training-free inference-time framework. OSCAR runs N parallel denoising chains with randomized reveal orders, computes cross-chain entropy to localize uncertainties, and performs targeted remarking with retrieved evidence. The pipeline requires only modest runtime increase while delivering substantial quality gains. OSCAR is positioned as the first training-free zero-shot DLM native hallucination detection and mitigation method.

Our work fully characterizes commitment uncertainty in diffusion language models, its origin, measurement, actions, and formation, organized into four contributions: (a) We identify and demonstrate a native uncertainty signal inherent in diffusion language models (DLMs), derived from cross-chain Shannon entropy computed across multiple parallel denoising trajectories with randomized reveal orders. This signal enables competitive hallucination detection without external supervision, highlighting an uncertainty measure structurally absent in autoregressive models. (b) We formalize the task of commitment uncertainty

localization by introducing the cross-chain divergence-at-hallucination (CDH) metric, which effectively identifies factually unreliable token positions within denoising trajectories, substantially outperforming baseline methods. (c) We propose OSCAR, the first inference-time hallucination mitigation framework for DLMs, which leverages targeted re-masking and re-denoising of uncertain token spans to correct hallucinations. OSCAR achieves significant improvements in generation quality and factual accuracy across multiple benchmarks while maintaining efficient computational overhead. (d) We provide a mechanistic analysis of hallucination crystallization timing during the denoising process, revealing task-dependent patterns that support early-exit detection strategies and enable adaptive, task-specific intervention.

2 Related Work

Hallucination detection in autoregressive (AR) language models has developed through three main approaches. Uncertainty-based methods estimate confidence by examining output token distributions (Malinin & Gales, 2021; Ren et al., 2023). Semantic entropy methods group equivalent outputs before calculating entropy to capture meaning-level uncertainty (Kuhn et al., 2023; Farquhar et al., 2024). Probe-based methods train lightweight classifiers on internal model activations to identify hallucinations (Azaria & Mitchell, 2023; Burns et al., 2024). SelfCheckGPT evaluates agreement across multiple generations but requires multiple generations and lacks correction mechanisms (Manakul et al., 2023). Evaluation has evolved, with ROUGE-based metrics shown inferior to LLM-as-Judge protocols, leading to combined evaluation approaches (Janiak et al., 2025). However, current methods do not address hallucination detection in diffusion language models (DLMs), which use parallel bidirectional denoising architecture, necessitating new DLM-specific approaches.

Hallucination detection in diffusion language models (DLMs) has recently gained attention as a promising area of research. Methods such as TraceDet model the denoising process as an action trace and identify the most informative sub-traces using the Information Bottleneck principle, resulting in a 15.2% average AUROC improvement over output-based baselines. DynHD tackles the issue of information density imbalance across token positions by constructing semantic-aware evidence and introducing a reference evidence generator that learns the expected uncertainty evolution, detecting hallucinations by measuring deviations from this reference. EigenScore (Shoushtari et al., 2025) leverages the eigenvalue spectrum of the posterior covariance induced by the diffusion model as an out-of-distribution (OOD) detection signal. While these approaches effectively use the denoising trajectory as diagnostic input for classification, they do not modify or control the denoising process itself. This limitation hinders adaptability, as the denoising trajectory remains a passive signal rather than an active means for correction.

Existing approaches can be viewed as restricted instantiations of a general principle: *disagreement among diverse generations reveals factual uncertainty*. Independent resampling (SelfCheckGPT (Manakul et al., 2023)) measures total output variance but conflates sampling noise with factual uncertainty because each resample traverses the full generation process independently. Trajectory classifiers (TraceDet, DynHD) learn to recognize hallucination-correlated patterns in the denoising trace but require labeled data and provide no correction affordance. Cross-chain entropy under reveal-order diversification isolates the *commitment-order* component of disagreement directly, the precise structural source of DLM hallucination, without training. OSCAR operationalizes this signal end-to-end: it transforms the denoising trajectory from a passive diagnostic input into an active control mechanism, enabling targeted correction at the positions where commitment uncertainty is highest.

3 OSCAR: Commitment Uncertainty Localization and Correction

We present OSCAR in four parts that mirror our contributions. We first identify the structural failure mode underlying hallucination in DLMs and show that it produces a measurable, model-native uncertainty signal (§3.1; contribution a). We then formalize the localization problem and introduce the CDH evaluation metric (§3.2; contribution b). We describe the

full detection-and-correction pipeline (§3.3; contribution c), and finally connect the signal’s temporal structure to hallucination crystallization dynamics (§3.4; contribution d).

3.1 A Native Uncertainty Signal in Diffusion Language Models

A DLM generates response $\mathbf{y} = (y_1, \dots, y_L)$ to query q through T denoising steps. At $t=0$ all positions are masked; at each step the model predicts $p_\theta(y_i | \mathbf{y}^{(t-1)}, q)$ and reveals a subset according to a *reveal order* π . The resulting states form a *denoising trajectory* $\tau^\pi = (\mathbf{y}^{(0)}, \dots, \mathbf{y}^{(T)})$. Standard inference uses a confidence-based order; LLaDA-8B (Nie et al., 2025) uses $T=128$ steps, Dream-7B (Ye et al., 2025) uses $T=64$.

Once revealed, a token is *committed*: all subsequent steps condition on it irreversibly. A factually incorrect early commitment acts as a *contextual attractor*, biasing neighbors toward internally consistent but wrong predictions via bidirectional attention (Chang et al., 2025; Qian et al., 2026). We call this *premature commitment hallucination*. Unlike autoregressive hallucination, confined to the generation frontier, a single early error propagates through all remaining denoising steps.

The key insight is that such hallucinations are *order-dependent*: a different reveal order $\pi' \neq \pi$ may commit a different token first, potentially yielding a correct output. Running N parallel chains with independently randomized reveal orders exposes this latent uncertainty without external supervision.

Definition 1 (Cross-Chain Entropy). Let $y_i^{(T,n)}$ denote the final token at position i from chain n . The empirical distribution is $\hat{p}_i(v) = \frac{1}{N} \sum_{n=1}^N \mathbb{1}[y_i^{(T,n)} = v]$. The **cross-chain entropy** at position i is:

$$H_{\times,i} = - \sum_{v \in \mathcal{V}} \hat{p}_i(v) \log \hat{p}_i(v) \quad (1)$$

Positions with $H_{\times,i}=0$ are *commitment-stable*: every chain agrees regardless of reveal order. Positions with high $H_{\times,i}$ are *commitment-uncertain*: the output depends on the arbitrary ordering rather than on factual knowledge. Position i is commitment-stable if all reveal orders yield the same token: $H_{\times,i} = 0$ characterizes this. Cross-chain entropy is the complete measure of commitment disagreement: zero when order-invariant, positive when reveal schedule affects output. This signal is *model-native*, from the DLM’s denoising dynamics without a trained classifier or labeled data, and *structurally specific to DLMs*; autoregressive generation needs full resamples, while DLMs use parallel chains to isolate effects. With token vocabulary $|\mathcal{V}|$ over 32,000, the mean distinct tokens per position across $N=8$ chains is 2.7 (median 1, max 8), ensuring reliable entropy estimation. Cross-chain entropy, as a standalone detection signal, outperforms trained trajectory classifiers, capturing factual uncertainty more directly (§5.1).

3.2 Localization Formulation and CDH Metric

We formalize the task of identifying factually unreliable positions from parallel denoising trajectories.

Definition 2 (Commitment Uncertainty Localization). Given query q and N trajectories $\{\tau^{\pi_n}\}_{n=1}^N$, identify:

$$\mathcal{U} = \{ i : H_{\times,i} > Q_{1-\alpha}(H_{\times,1:L}) \} \quad (2)$$

where $Q_{1-\alpha}$ is the $(1-\alpha)$ -quantile of the entropy distribution (default localization aggressiveness threshold $(\alpha)=0.2$, flagging the top 20% most uncertain positions).

This formulation is (1) **training-free**: $Q_{1-\alpha}$ is computed from the current sample, requiring no labeled data; (2) **model-native**: the signal originates entirely from the DLM’s denoising process; and (3) **pre-correction**: uncertainty is measured from N parallel chains before any modification, avoiding post-hoc circularity.

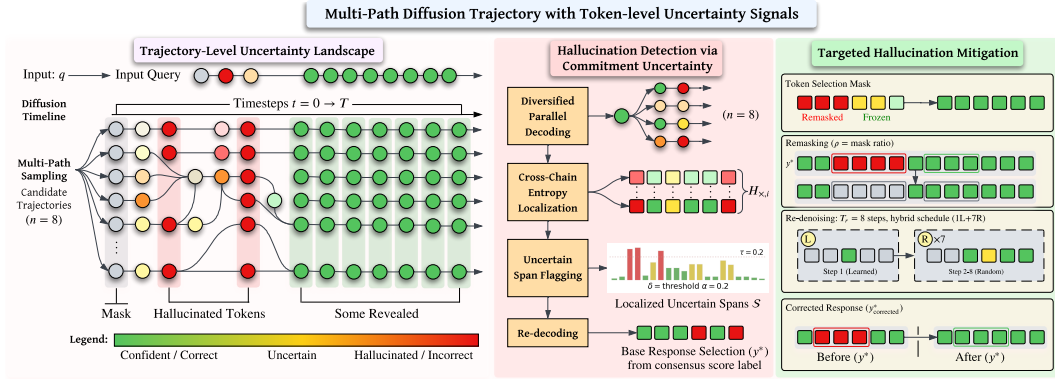


Figure 2: OSCAR overview. Phase 1: N parallel denoising chains with randomized reveal orders generate diverse trajectories. Cross-chain entropy H_{\times} identifies high-uncertainty positions (red). Phase 2: targeted remasking, conditioned on retrieved evidence, corrects hallucinated spans at $1.3\times$ overhead.

To evaluate localization quality at the token level, we introduce the *cross-chain divergence-at-hallucination rate*:

$$\text{CDH}(k) = \frac{|\{i \in \mathcal{U}_k : i \text{ is hallucinated}\}|}{|\{i : i \text{ is hallucinated}\}|} \quad (3)$$

where \mathcal{U}_k contains positions with the top- $k\%$ highest $H_{\times,i}$. $\text{CDH}(k)$ measures the fraction of truly hallucinated positions captured by the top- $k\%$ most uncertain positions (random baseline: $k/100$). Because OSCAR’s correction acts on localized spans, CDH directly measures the signal driving mitigation performance. We show in §5.3 that cross-chain entropy concentrates hallucinated positions in the high-uncertainty tail far more effectively than both random selection and the strongest trained alternative, confirming that unsupervised localization from the model’s own trajectories is sufficient for targeted correction.

3.3 The OSCAR Pipeline

Before detailing the pipeline, note that OSCAR implements a program for commitment uncertainty localization in DLMs: **(1)** diversify reveal orders to expose latent factual uncertainty; **(2)** compute a position-level disagreement statistic from trajectories; **(3)** threshold to localize uncertain spans; **(4)** correct via targeted re-denoising conditioned on context or evidence. OSCAR uses cross-chain Shannon entropy as the disagreement statistic, but alternatives like token-level KL divergence or embedding-space distance are possible. The correction stage could use stronger evidence sources or iterative refinement. We present choices yielding the strongest empirical results; the general program is the conceptual contribution. OSCAR operationalizes commitment uncertainty localization in three stages (Figure 2).

Stage 1: Diversified parallel decoding. OSCAR samples N reveal orders uniformly at random and runs N chains in parallel, sharing model weights θ . Standard confidence-based decoding always commits the most confident predictions first, suppressing observable uncertainty via contextual attractors (§3.1). Randomized orders break this coupling, ensuring no position receives systematic priority. All chains are batched into a single forward pass per step, yielding approximately one and a fifth times additional processing time.

Stage 2: Localization and span aggregation. OSCAR computes $H_{\times,i}$ (Eq. 1) at each position and applies the percentile threshold (Eq. 2) to obtain the uncertain set \mathcal{U} . Consecutive positions are grouped into spans, each extended by $w=2$ tokens on either side; spans shorter than $\ell_{\min}=3$ tokens are discarded (ablated in Appendix B.2). The base response y^* is the chain whose tokens best match the cross-chain consensus:

$$n^* = \arg \max_n \sum_{i=1}^L \hat{p}_i(y_i^{(T,n)}) \quad (4)$$

Stage 3: Targeted remasking and correction. For each span $s = (a, \dots, b) \in \mathcal{S}$, OSCARremasks positions a through b in \mathbf{y}^* and runs T_r denoising steps with all surrounding tokens frozen:

$$\hat{\mathbf{y}}_s = \arg \max_{\mathbf{y}_{a:b}} p_{\theta}(\mathbf{y}_{a:b} \mid \mathbf{y}_{\setminus s}^*, [\mathbf{e}_s; q]) \quad \text{via } T_r \text{ denoising steps} \quad (5)$$

where \mathbf{e}_s is optional retrieved evidence. This exploits the DLM’s native ability to fill masked regions given surrounding context, an affordance unavailable in autoregressive models.

The first refinement step uses the learned confidence-based order, anchoring the correction with the most confident prediction to prevent a new attractor. The remaining $T_r - 1$ steps use random orders, allowing the span to settle without reproducing the original error. When a retrieval corpus is available, the uncertain span text serves as the query (rather than the full input), focusing evidence on the specific claim under correction. We use Contriever (Izacard et al., 2022) over a 2021 Wikipedia snapshot (top-1 passage, 256 tokens).

Overhead and hyperparameters. The correction stage remasks $\sim 18.7\%$ of tokens on average. With $T_r=8$ steps and batched inference, correction adds $\sim 0.1\times$; combined with diversification ($\sim 1.2\times$), total overhead is $\sim 1.3\times$. Defaults: $N=8$ chains, $\alpha=0.2$, $T_r=8$, $w=2$, $\ell_{\min}=3$, 1-Learned + (T_r-1) -Random schedule. Each is validated by ablations in later sections.

3.4 Crystallization: When Do Hallucinations Form?

The cross-chain entropy signal is not only diagnostic of *where* hallucinations occur but also *when* they form during denoising. We define the *entropy gap* at step t as the difference in mean cross-chain entropy between hallucinated and grounded positions:

$$\Delta H(t) = \mathbb{E}[H_{\times} \mid \text{hallucinated}, t] - \mathbb{E}[H_{\times} \mid \text{grounded}, t] \quad (6)$$

We find $\Delta H(t)$ ’s temporal profile is task-dependent. In factual QA, the entropy gap peaks early and persists, showing factual uncertainty crystallizes quickly. For summarization, the gap grows mid-denoising, reflecting compositional errors. In factual QA, an early incorrect commitment dominates due to bidirectional attention. In summarization, hallucinations from compositional choices across spans require more denoising to detect cross-chain disagreement. Token-level ground truth uses RAGTruth’s span annotations; for TriviaQA, we align the final gold answer against each intermediate state via exact-match at each step. This crystallization pattern supports OSCAR as diverse reveal orders are informative when commitment-order effects are strongest, suggesting early-exit detection to reduce overhead (full analysis in §6.3).

4 Experimental Setup

Models and datasets. We evaluate on LLaDA-8B-Instruct (Nie et al., 2025) ($T=128$ steps) and Dream-7B-Instruct (Ye et al., 2025) ($T=64$). Benchmarks: TriviaQA (Joshi et al., 2017) (500), HotpotQA (Yang et al., 2018) (500), CommonsenseQA (Talmor et al., 2019) (500; negative control—multiple-choice format yields $H_{\times} \approx 0$), and RAGTruth (Niu et al., 2024) (500; token-level span annotations).

Baselines and evaluation. Nine baselines across three families: output-based (Perplexity, LN-Entropy, Semantic Entropy (Kuhn et al., 2023; Farquhar et al., 2024), Lexical Similarity (Manakul et al., 2023)), latent-based (EigenScore (Shoushtari et al., 2025), CCS (Burns et al., 2024), TSV (Chang et al., 2025)), and trajectory-based (TraceDet (Chang et al., 2025), DynHD (Qian et al., 2026)), plus token-level majority vote across $N=8$ chains. We report AUROC under EM and LLM-as-Judge (GPT-4o (OpenAI et al., 2024)), F1 before/after correction, CDH(k), and span reduction on RAGTruth (Niu et al., 2024); all as mean \pm std over three seeds. Defaults: $N=8$, $\alpha=0.2$, $T_r=8$; batched on $4\times$ H200 80GB; retrieval via Contriever (Izacard et al., 2022) over Wikipedia.

5 Discussion

5.1 Hallucination Detection: OSCAR Surpasses Trained Detectors

Table 1 presents AUROC results. Under LLM-as-Judge evaluation, OSCAR achieves **86.5%** average AUROC on LLaDA-8B and **85.7%** on Dream-7B—surpassing DynHD (the strongest trained detector) by **+2.3** and **+1.4** points respectively. Under exact-match evaluation, OSCAR scores 76.4% (LLaDA-8B), which is lower than DynHD’s 84.2% because EM penalizes OSCAR’s semantically correct but lexically different corrections.

The **+10.7 AUROC gain** reflects the gap between OSCAR’s raw entropy signal-localization only, without correction, and TraceDet (82.7 vs. 72.0 on LLaDA-8B).² This gain is achieved *without any hallucination-specific training*, revealing that the cross-chain entropy signal captures factual uncertainty more effectively than trained trajectory classifiers.

5.2 Generation Quality and Span Correction

Figure 3 shows F1 scores before and after correction. OSCAR improves QA macro-average F1 by +6.1 pp on LLaDA-8B and +8.3 pp across both models, with the largest gain in TriviaQA (+10.7). In CommonsenseQA, $\Delta F1 = 0.0$ as chains agree on single-token answers ($H_x \approx 0$), so OSCAR doesn’t intervene. The strong sample-level AUROC on CommonsenseQA shows high confidence outputs ($H_x \approx 0$) are factual; position-level $H_x \approx 0$ indicates no uncertain spans to correct, these signals are complementary, not contradictory. Results for Dream-7B show similar improvements. Figure 4 shows OSCAR’s correction extends beyond short-form QA: hallucinated spans decrease 38–44% across RAGTruth subsets, with positive ΔFS showing improved factual precision. Uncertainty-targeted retrieval adds +3.4 F1 over OSCAR (Appendix A.1).

5.3 Localization Quality: CDH Analysis

Appendix A.2 reports CDH(k) curves. At $k=20\%$ (i.e., examining only the top 20% most uncertain positions), OSCAR’s cross-chain entropy captures 67.3% of all hallucinated positions on LLaDA-8B—more than $3\times$ the random baseline (20%) and $1.4\times$ the best trained detector

²The entropy-only AUROC uses cross-chain entropy \mathcal{H}_x as the detection score directly, without the correction stage. With correction and LLM-as-Judge relabeling, the full-pipeline AUROC rises further to 86.5%.

Method		TriviaQA		HotpotQA		CSQA		Avg
		128	64	128	64	128	64	
<i>LLaDA-8B-Instruct</i>								
Output	Perplexity	50.4	47.6	49.3	51.2	65.6	65.0	54.9
	LN-Entropy	54.6	53.5	54.8	54.7	64.6	64.4	57.8
	Semantic Entropy	68.9	67.3	57.6	53.8	44.1	43.9	55.9
	Lexical Similarity	62.5	59.0	64.2	57.1	57.3	60.7	60.1
Latent	EigenScore	69.2	66.9	64.7	59.2	58.5	60.6	63.2
	CCS	57.1	54.2	57.6	55.8	50.5	58.5	55.6
	TSV	60.2	61.1	65.0	59.4	52.9	55.2	59.0
Traj.	TraceDet [†]	73.9	74.1	66.1	63.7	77.2	77.1	72.0
	DynHD [†]	86.7	86.1	84.2	85.3	81.6	81.3	84.2
	OSCAR (EM)	80.3	79.8	71.5	68.2	79.4	78.9	76.4
	OSCAR (Judge)	89.7	88.8	86.7	87.5	83.4	82.8	86.5
<i>Dream-7B-Instruct</i>								
Out.	Semantic Entropy	73.7	72.5	62.7	67.7	51.4	48.6	62.8
	Lexical Similarity	58.3	64.0	59.7	62.7	77.3	76.9	66.5
Lat.	EigenScore	66.0	69.1	62.5	67.0	76.9	77.5	69.8
	CCS	56.9	50.3	51.7	58.2	54.2	53.2	54.1
	TSV	75.6	74.7	58.7	63.0	62.3	56.8	65.2
Traj.	TraceDet [†]	78.1	86.7	75.1	76.0	84.7	84.1	80.8
	DynHD [†]	87.3	84.4	80.1	85.6	83.5	84.6	84.3
	OSCAR (EM)	82.6	83.1	77.4	79.8	84.2	83.7	81.8
	OSCAR (Judge)	89.5	86.3	81.9	87.1	84.3	85.1	85.7

[†] = requires trained classifier on hallucination labels. Also uses LLM-as-Judge eval

Table 1: AUROC(%) on two DLMs across three QA datasets. Best **bolded**, second underlined. Green = OSCAR (EM eval). Blue = OSCAR (LLM-as-Judge eval). All trained baselines use EM labels only.

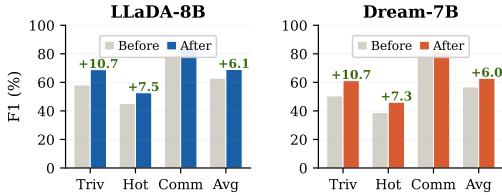


Figure 3: F1 before (gray) and after (color) OSCAR correction. Green annotations show $\Delta F1$. CommonsenseQA shows no change ($H_{\times} \approx 0$), validating selectivity. Mean \pm std over 3 seeds; full metrics in Appendix B.4.

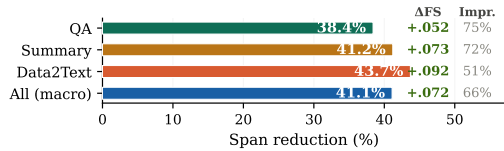


Figure 4: Span-level correction on RAGTruth (LLaDA-8B). Bars show hallucinated span reduction; ΔFS and % Improved annotated at right. Full per-subset metrics in Appendix A.

(TraceDet, 47.8%). This validates that cross-chain entropy is a highly effective localization signal without requiring any supervision.

5.4 Pareto Analysis: Performance vs. Efficiency

Figure 5 presents the Pareto frontier. OSCAR (with Judge evaluation) achieves the highest AUROC at $1.3\times$ wall-clock overhead, establishing a new Pareto-optimal point that encompasses both hallucination mitigation and detection. The key insight: even with $N=8$ parallel chains, batched inference keeps the overhead manageable, while the detection + correction synergy produces gains that neither component achieves alone.

6 Ablation and Analysis

We decompose OSCAR’s gains to identify which components are load-bearing, how sensitive the method is to its control parameters, and why cross-chain entropy is an effective uncertainty signal.

6.1 Localization and Correction are Complementary

Table 2 shows that localization alone does not affect F1 performance, while random span corrections slightly reduce results. The complete OSCAR pipeline integrates localization with targeted correction, achieving a 6.1-point F1 improvement and 86.5 AUROC, outperforming untargeted correction (+2.5 F1) and token-level majority voting (+2.2 F1). Table 3 shows the default OSCAR configuration (1L+7R) outperforms alternative ordering schemes across all

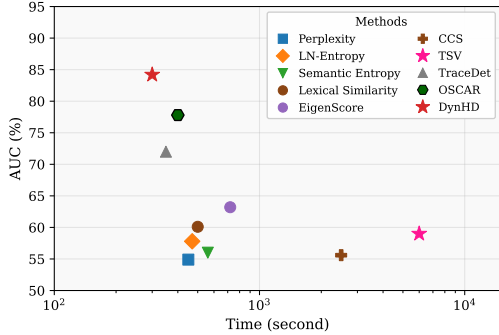


Figure 5: **Pareto frontier.** AUC = LLaDA-8B average. \star = Pareto-optimal. Wall-clock on $4\times H200$.

Configuration	F1 (%)	AUROC	$\Delta F1$
Unguided decoding	62.9	—	—
Best-of-N selection (no correction)	62.9	82.7	+0.0
Correction only (random spans)	62.8	—	-0.1
Majority vote — token	65.1	—	+2.2
Localization + untargeted correction	65.4	83.1	+2.5
OSCAR (loc. + targeted)	69.0	86.5[†]	+6.1

[†] Under LLM-as-Judge. EM-eval AUROC = 76.4.

Table 2: **Complementarity ablation** (LLaDA-8B, QA macro-avg). Localization-only AUROC = 82.7 (raw entropy signal, no correction).

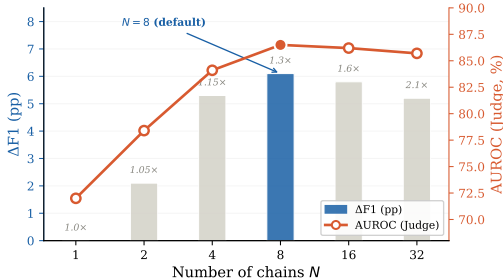
Order	Triv. F1	CQ F1	HQA F1	RT R-L	AUROC	Avg F1
All learned	56.8	85.4	43.1	33.8	0.541	61.8
All random	61.2	85.4	47.3	37.4	0.608	64.6
Hybrid (50/50)	64.8	85.4	49.8	40.1	0.627	66.7
Entropy-ordered	59.4	85.4	44.7	35.2	0.591	63.2
OSCAR (1L+7R)	68.9	85.4	52.7	43.2	0.639	69.0

Table 3: Demasking order ablation (LLaDA-8B). OSCAR default = 1L+7R.

metrics. These results demonstrate the synergy between localization and targeted correction within OSCAR, validating its ability to enhance model output quality.

6.2 Sensitivity Analysis

Figure 6 shows the effect of chains $N \in \{1, 2, 4, 8, 16, 32\}$ on LLaDA-8B (QA macro-avg), where F1 gain and AUROC increase from $N = 1$ to $N = 4$, peak at $N = 8$, and plateau at $N = 16$ – 32 ; thus, $N = 8$ provides optimal localization quality versus cost. For demasking order, the hybrid schedule (one learned step followed by $(T_r - 1)$ random steps) outperforms alternatives: all-learned achieves 61.8 F1 (below 62.9 baseline), all-random reaches 64.6, and entropy-ordered yields 63.2. The learned step anchors the most confident token, while random steps add diversity as in Table 3. OSCAR corrections show 91–97% precision in improving outputs (57 vs. 5 on TriviaQA, 34 vs. 1 on HotpotQA; Appendix B.1). The threshold α shows optimal F1 in $[0.15, 0.25]$ across $\{0.05, 0.10, \dots, 0.40\}$, degrading at extremes (Appendix B.2).

Figure 6: Effect of chains N on LLaDA-8B (QA macro-avg).

6.3 Why Does Cross-Chain Entropy Work?

Cross-chain entropy leverages the architectural difference between autoregressive (AR) and diffusion language models (DLMs). In AR decoding, uncertainty at position i is hidden at $i + 1$ since only the argmax token propagates, collapsing the distribution. Recovering uncertainty requires independent resamples, mixing sampling variance with factual uncertainty. DLMs maintain the full probability distribution, sampling various paths via different reveal orders. Cross-chain entropy measures the width of this path distribution at each position, capturing a factual uncertainty signal absent in AR models. This unsupervised signal from $N = 8$ DLM chains outperforms trained classifiers reconstructing commitment uncertainty from trajectory features, confirmed by ablations. Unlike TraceDet and DynHD, which learn from hallucination labels, cross-chain entropy directly measures this signal, surpassing trained classifiers without supervision. Confident-but-wrong cases, where chains agree on incorrect answers ($H_{\times} = 0$), represent 9–20% of hallucinated positions (Appendix B.3), indicating a need for retrieval augmentation rather than remasking, as shown by zero-entropy readout.

7 Conclusion

We introduced commitment uncertainty localization to identify unreliable token positions from diffusion language models’ denoising trajectories, formalized through the CDH metric. OSCAR, our training-free framework, runs N parallel chains with randomized reveal orders, computes cross-chain entropy to localize unstable positions, and corrects them via targeted remasking. On LLaDA-8B and Dream-7B, OSCAR improves F1 by $+8.3 \pm 0.4$, reduces hallucinated spans by 41.1%, and achieves 86.5 AUROC, surpassing trained classifiers

at $1.3\times$ overhead. The signal’s effectiveness stems from a structural asymmetry: DLMs maintain full distributions throughout denoising, exposing commitment-order effects that AR models collapse at each step. Crystallization analysis reveals task-dependent timing, supporting early-exit detection for reducing overhead. Our findings demonstrate that diffusion language models contain native uncertainty signals enabling both error localization and correction during inference—an affordance absent in autoregressive generation.

Future work. Several directions follow naturally from this work. First, the crystallization analysis suggests that much of the useful uncertainty signal emerges in the earliest denoising steps; this raises the possibility of early-exit detection and lower-cost correction schedules. Second, extending commitment uncertainty localization beyond discrete masked diffusion to continuous or hybrid diffusion language models would test how general the signal is across architectures. Third, adaptive intervention policies—including task-dependent thresholds α , span-selection strategies, or correction schedules—may improve the accuracy–efficiency trade-off further. Finally, integrating OSCAR-style localization with preference optimization, retrieval planning, or external tool use could broaden its role from factual repair to more general inference-time control. We release the trajectory divergence toolkit to support future work on localization, correction, and uncertainty-aware generation in DLMs.

Limitations

Five limitations bound the current work. (1) OSCAR requires running N parallel chains, increasing peak VRAM by $\sim 1.67\times$ for $N=8$ (32.1 GB vs. 19.2 GB) even though wall-clock time only increases $1.3\times$ via batching. (2) For queries where the model lacks relevant knowledge entirely, correction via remasking cannot help—the model will hallucinate consistently across all chains. (3) The LLM-as-Judge evaluation introduces its own biases. (4) We evaluate two DLMs; generalization to future architectures is not guaranteed. (5) Span aggregation hyperparameters (± 2 token extension, 3-token minimum) are validated empirically but not theoretically grounded.

Ethics Statement

This work proposes training-free inference-time techniques for reducing hallucination in diffusion language models. We do not introduce new training data, fine-tuned models, or large-scale data collection. The models evaluated (LLaDA-8B, Dream-7B) are publicly available research artifacts; evaluations use public benchmarks (TriviaQA, HotpotQA, CommonsenseQA, RAGTruth). LLaDA-8B and Dream-7B are the only publicly available DLMs at scale as of early 2026; our evaluation therefore covers the full available ecosystem. Technical limitations—including computational overhead, failure modes under complete knowledge absence, evaluation biases, and hyperparameter sensitivity—are detailed in §7. The LLM-as-Judge evaluation (GPT-4o) introduces potential biases; no human evaluation of user-perceived helpfulness is included. GPT-4o assisted in polishing this manuscript; associated costs and biases are acknowledged.

References

- Amos Azaria and Tom Mitchell. The Internal State of an LLM Knows When It’s Lying, October 2023. URL <http://arxiv.org/abs/2304.13734>. arXiv:2304.13734 [cs].
- Benjamin Bloem-Reddy and Yee Whye Teh. Probabilistic symmetries and invariant neural networks. *J. Mach. Learn. Res.*, 21(1):90:3535–90:3595, January 2020. ISSN 1532-4435. URL <https://dl.acm.org/doi/10.5555/3455716.3455806>.
- Collin Burns, Haotian Ye, Dan Klein, and Jacob Steinhardt. Discovering Latent Knowledge in Language Models Without Supervision, March 2024. URL <http://arxiv.org/abs/2212.03827>. arXiv:2212.03827 [cs].

- Shenxu Chang, Junchi Yu, Weixing Wang, Yongqiang Chen, Jialin Yu, Philip Torr, and Jindong Gu. TraceDet: Hallucination Detection from the Decoding Trace of Diffusion Large Language Models, September 2025. URL <http://arxiv.org/abs/2510.01274>. arXiv:2510.01274 [cs].
- Chao Chen, Kai Liu, Ze Chen, Yi Gu, Yue Wu, Mingyuan Tao, Zhihang Fu, and Jieping Ye. INSIDE: LLMs’ Internal States Retain the Power of Hallucination Detection, February 2024. URL <http://arxiv.org/abs/2402.03744>. arXiv:2402.03744 [cs].
- Sebastian Farquhar, Jannik Kossen, Lorenz Kuhn, and Yarin Gal. Detecting hallucinations in large language models using semantic entropy. *Nature*, 630(8017):625–630, June 2024. ISSN 1476-4687. doi: 10.1038/s41586-024-07421-0. URL <https://www.nature.com/articles/s41586-024-07421-0>.
- Gautier Izacard, Mathilde Calmès, Lucas Huot, Fabio Petroni, Mike Lewis, Sarath Chandar, Sebastian Riedel, and Edouard Grave. Unsupervised Dense Information Retrieval with Contrastive Learning. *Transactions on Machine Learning Research*, 2022. doi: 10.48550/arXiv.2112.09118. URL <http://arxiv.org/abs/2112.09118>. arXiv:2112.09118 [cs].
- Denis Janiak, Jakub Binkowski, Albert Sawczyn, Bogdan Gabrys, Ravid Shwartz-Ziv, and Tomasz Kajdanowicz. The Illusion of Progress: Re-evaluating Hallucination Detection in LLMs, August 2025. URL <http://arxiv.org/abs/2508.08285>. arXiv:2508.08285 [cs].
- Mandar Joshi, Eunsol Choi, Daniel S. Weld, and Luke Zettlemoyer. TriviaQA: A Large Scale Distantly Supervised Challenge Dataset for Reading Comprehension, May 2017. URL <http://arxiv.org/abs/1705.03551>. arXiv:1705.03551 [cs].
- Lorenz Kuhn, Yarin Gal, and Sebastian Farquhar. Semantic Uncertainty: Linguistic Invariances for Uncertainty Estimation in Natural Language Generation, April 2023. URL <http://arxiv.org/abs/2302.09664>. arXiv:2302.09664 [cs].
- Patrick Lewis, Ethan Perez, Aleksandra Piktus, Fabio Petroni, Vladimir Karpukhin, Naman Goyal, Heinrich Küttler, Mike Lewis, Wen-tau Yih, Tim Rocktäschel, et al. Retrieval-Augmented Generation for Knowledge-Intensive NLP Tasks. In *Advances in Neural Information Processing Systems*, volume 33, pp. 9459–9474, 2020.
- Tianyi Li, Mingda Chen, Bowei Guo, and Zhiqiang Shen. A Survey on Diffusion Language Models, August 2025. URL <http://arxiv.org/abs/2508.10875>. arXiv:2508.10875 [cs].
- Zhen Lin, Shubhendu Trivedi, and Jimeng Sun. Generating with Confidence: Uncertainty Quantification for Black-Box Large Language Models. *Transactions on Machine Learning Research*, 2024. URL <https://api.semanticscholar.org/CorpusID:258967487>.
- Rui Lu, Runzhe Wang, Kaifeng Lyu, Xitai Jiang, Gao Huang, and Mengdi Wang. Towards Understanding Text Hallucination of Diffusion Models via Local Generation Bias. October 2024. URL <https://openreview.net/forum?id=SKW10XJ1AI>.
- Andrey Malinin and Mark Gales. Uncertainty Estimation in Autoregressive Structured Prediction, February 2021. URL <http://arxiv.org/abs/2002.07650>. arXiv:2002.07650 [stat].
- Potsawee Manakul, Ada Wang, and Mark J.F. Gales. SelfCheckGPT: Zero-Resource Black-Box Hallucination Detection for Generative Large Language Models. In Houda Bouamor, Juan Pino, and Kalika Bali (eds.), *Proceedings of the 2023 Conference on Empirical Methods in Natural Language Processing*, pp. 9004–9017, Singapore, December 2023. Association for Computational Linguistics. doi: 10.18653/v1/2023.emnlp-main.557. URL <https://aclanthology.org/2023.emnlp-main.557>. arXiv:2303.08896 [cs].
- Sewon Min, Kalpesh Krishna, Xixi Lyu, Mike Lewis, Wen-tau Yih, Pang Wei Koh, Mohit Iyyer, Luke Zettlemoyer, and Hannaneh Hajishirzi. FActScoring: Fine-Grained Atomic Evaluation of Factual Precision in Long Form Text Generation. In Houda Bouamor, Juan Pino, and Kalika Bali (eds.), *Proceedings of the 2023 Conference on Empirical Methods in Natural Language Processing*, pp. 12076–12100, Singapore, December 2023. Association

for Computational Linguistics. doi: 10.18653/v1/2023.emnlp-main.741. URL <https://aclanthology.org/2023.emnlp-main.741>. arXiv:2305.14251 [cs].

Shen Nie, Fengqi Zhu, Zebin You, Xiaolu Zhang, Jingyang Ou, Jun Hu, Jun Zhou, Yankai Lin, Ji-Rong Wen, and Chongxuan Li. Large Language Diffusion Models, October 2025. URL <http://arxiv.org/abs/2502.09992>. arXiv:2502.09992 [cs].

Cheng Niu, Yuanhao Wu, Juno Zhu, Siliang Xu, KaShun Shum, Randy Zhong, Juntong Song, and Tong Zhang. RAGTruth: A Hallucination Corpus for Developing Trustworthy Retrieval-Augmented Language Models. In Lun-Wei Ku, Andre Martins, and Vivek Srikumar (eds.), *Proceedings of the 62nd Annual Meeting of the Association for Computational Linguistics (Volume 1: Long Papers)*, pp. 10862–10878, Bangkok, Thailand, August 2024. Association for Computational Linguistics. doi: 10.18653/v1/2024.acl-long.585. URL <https://aclanthology.org/2024.acl-long.585/>.

OpenAI, Josh Achiam, Steven Adler, Sandhini Agarwal, Lama Ahmad, Ilge Akkaya, Florenzia Leoni Aleman, Diogo Almeida, Janko Altenschmidt, Sam Altman, Shyamal Anadkat, Red Avila, Igor Babuschkin, Suchir Balaji, Valerie Balcom, Paul Baltescu, Haiming Bao, Mohammad Bavarian, Jeff Belgum, Irwan Bello, Jake Berdine, Gabriel Bernadett-Shapiro, Christopher Berner, Lenny Bogdonoff, Oleg Boiko, Madelaine Boyd, Anna-Luisa Brakman, Greg Brockman, Tim Brooks, Miles Brundage, Kevin Button, Trevor Cai, Rosie Campbell, Andrew Cann, Brittany Carey, Chelsea Carlson, Rory Carmichael, Brooke Chan, Che Chang, Fotis Chantzis, Derek Chen, Sully Chen, Ruby Chen, Jason Chen, Mark Chen, Ben Chess, Chester Cho, Casey Chu, Hyung Won Chung, Dave Cummings, Jeremiah Currier, Yunxing Dai, Cory Decareaux, Thomas Degry, Noah Deutsch, Damien Deville, Arka Dhar, David Dohan, Steve Dowling, Sheila Dunning, Adrien Ecoffet, Atty Eleti, Tyna Eloundou, David Farhi, Liam Fedus, Niko Felix, Simón Posada Fishman, Juston Forte, Isabella Fulford, Leo Gao, Elie Georges, Christian Gibson, Vik Goel, Tarun Gogineni, Gabriel Goh, Rapha Gontijo-Lopes, Jonathan Gordon, Morgan Grafstein, Scott Gray, Ryan Greene, Joshua Gross, Shixiang Shane Gu, Yufei Guo, Chris Hallacy, Jesse Han, Jeff Harris, Yuchen He, Mike Heaton, Johannes Heidecke, Chris Hesse, Alan Hickey, Wade Hickey, Peter Hoeschele, Brandon Houghton, Kenny Hsu, Shengli Hu, Xin Hu, Joost Huizinga, Shantanu Jain, Shawn Jain, Joanne Jang, Angela Jiang, Roger Jiang, Haozhun Jin, Denny Jin, Shino Jomoto, Billie Jonn, Heewoo Jun, Tomer Kaftan, Łukasz Kaiser, Ali Kamali, Ingmar Kanitscheider, Nitish Shirish Keskar, Tabarak Khan, Logan Kilpatrick, Jong Wook Kim, Christina Kim, Yongjik Kim, Jan Hendrik Kirchner, Jamie Kiros, Matt Knight, Daniel Kokotajlo, Łukasz Kondraciuk, Andrew Kondrich, Aris Konstantinidis, Kyle Kosic, Gretchen Krueger, Vishal Kuo, Michael Lampe, Ikai Lan, Teddy Lee, Jan Leike, Jade Leung, Daniel Levy, Chak Ming Li, Rachel Lim, Molly Lin, Stephanie Lin, Mateusz Litwin, Theresa Lopez, Ryan Lowe, Patricia Lue, Anna Makanju, Kim Malfacini, Sam Manning, Todor Markov, Yaniv Markovski, Bianca Martin, Katie Mayer, Andrew Mayne, Bob McGrew, Scott Mayer McKinney, Christine McLeavey, Paul McMillan, Jake McNeil, David Medina, Aalok Mehta, Jacob Menick, Luke Metz, Andrey Mishchenko, Pamela Mishkin, Vinnie Monaco, Evan Morikawa, Daniel Mossing, Tong Mu, Mira Murati, Oleg Murk, David Mély, Ashvin Nair, Reiichiro Nakano, Rajeev Nayak, Arvind Neelakantan, Richard Ngo, Hyeonwoo Noh, Long Ouyang, Cullen O’Keefe, Jakub Pachocki, Alex Paino, Joe Palermo, Ashley Pantuliano, Giambattista Parascandolo, Joel Parish, Emy Parparita, Alex Passos, Mikhail Pavlov, Andrew Peng, Adam Perelman, Filipe de Avila Belbute Peres, Michael Petrov, Henrique Ponde de Oliveira Pinto, Michael, Pokorny, Michelle Pokrass, Vitchyr H. Pong, Tolly Powell, Alethea Power, Boris Power, Elizabeth Proehl, Raul Puri, Alec Radford, Jack Rae, Aditya Ramesh, Cameron Raymond, Francis Real, Kendra Rimbach, Carl Ross, Bob Rotsted, Henri Roussez, Nick Ryder, Mario Saltarelli, Ted Sanders, Shibani Santurkar, Girish Sastry, Heather Schmidt, David Schnurr, John Schulman, Daniel Selsam, Kyla Sheppard, Toki Sherbakov, Jessica Shieh, Sarah Shoker, Pranav Shyam, Szymon Sidor, Eric Sigler, Maddie Simens, Jordan Sitkin, Katarina Slama, Ian Sohl, Benjamin Sokolowsky, Yang Song, Natalie Staudacher, Felipe Petroski Such, Natalie Summers, Ilya Sutskever, Jie Tang, Nikolas Tezak, Madeleine B. Thompson, Phil Tillet, Amin Tootoonchian, Elizabeth Tseng, Preston Tuggle, Nick Turley, Jerry Tworek, Juan Felipe Cerón Uribe, Andrea Vallone, Arun Vijayvergiya, Chelsea Voss, Carroll Wainwright, Justin Jay Wang, Alvin Wang, Ben Wang, Jonathan Ward, Jason Wei, C. J. Weinmann,

- Akila Welihinda, Peter Welinder, Jiayi Weng, Lilian Weng, Matt Wiethoff, Dave Willner, Clemens Winter, Samuel Wolrich, Hannah Wong, Lauren Workman, Sherwin Wu, Jeff Wu, Michael Wu, Kai Xiao, Tao Xu, Sarah Yoo, Kevin Yu, Qiming Yuan, Wojciech Zaremba, Rowan Zellers, Chong Zhang, Marvin Zhang, Shengjia Zhao, Tianhao Zheng, Juntang Zhuang, William Zhuk, and Barret Zoph. GPT-4 Technical Report, March 2024. URL <http://arxiv.org/abs/2303.08774>. arXiv:2303.08774 [cs].
- Seongheon Park, Xuefeng Du, Min-Hsuan Yeh, Haobo Wang, and Yixuan Li. Steer LLM Latents for Hallucination Detection. In *Proceedings of the 42nd International Conference on Machine Learning*, 2025. URL <https://api.semanticscholar.org/CorpusID:276767803>.
- Yanyu Qian, Yue Tan, Yixin Liu, Wang Yu, and Shirui Pan. DynHD: Hallucination Detection for Diffusion Large Language Models via Denoising Dynamics Deviation Learning, March 2026. URL <http://arxiv.org/abs/2603.16459>. arXiv:2603.16459 [cs].
- Jie Ren, Jiaming Luo, Yao Zhao, Kundan Krishna, Mohammad Saleh, Balaji Lakshminarayanan, and Peter J. Liu. Out-of-Distribution Detection and Selective Generation for Conditional Language Models, March 2023. URL <http://arxiv.org/abs/2209.15558>. arXiv:2209.15558 [cs].
- Shirin Shoushtari, Yi Wang, Xiao Shi, M. Salman Asif, and Ulugbek S. Kamilov. EigenScore: OOD Detection using Covariance in Diffusion Models, October 2025. URL <http://arxiv.org/abs/2510.07206>. arXiv:2510.07206 [cs] version: 1.
- Alon Talmor, Jonathan Herzig, Nicholas Lourie, and Jonathan Berant. CommonsenseQA: A Question Answering Challenge Targeting Commonsense Knowledge. In Jill Burstein, Christy Doran, and Thamar Solorio (eds.), *Proceedings of the 2019 Conference of the North American Chapter of the Association for Computational Linguistics: Human Language Technologies, Volume 1 (Long and Short Papers)*, pp. 4149–4158, Minneapolis, Minnesota, June 2019. Association for Computational Linguistics. doi: 10.18653/v1/N19-1421. URL <https://aclanthology.org/N19-1421/>.
- S. M. Towhidul Islam Tonmoy, S. M. Mehedi Zaman, Vinija Jain, Anku Rani, Vipula Rawte, Aman Chadha, and Amitava Das. A Comprehensive Survey of Hallucination Mitigation Techniques in Large Language Models, January 2024. URL <http://arxiv.org/abs/2401.01313>. arXiv:2401.01313 [cs].
- Ashish Vaswani, Noam Shazeer, Niki Parmar, Jakob Uszkoreit, Llion Jones, Aidan N. Gomez, Łukasz Kaiser, and Illia Polosukhin. Attention Is All You Need. In *Advances in Neural Information Processing Systems*, volume 30. Curran Associates, Inc., 2017.
- Zhilin Yang, Peng Qi, Saizheng Zhang, Yoshua Bengio, William Cohen, Ruslan Salakhutdinov, and Christopher D. Manning. HotpotQA: A Dataset for Diverse, Explainable Multi-hop Question Answering. In Ellen Riloff, David Chiang, Julia Hockenmaier, and Jun’ichi Tsujii (eds.), *Proceedings of the 2018 Conference on Empirical Methods in Natural Language Processing*, pp. 2369–2380, Brussels, Belgium, October 2018. Association for Computational Linguistics. doi: 10.18653/v1/D18-1259. URL <https://aclanthology.org/D18-1259/>.
- Jiacheng Ye, Zhihui Xie, Lin Zheng, Jiahui Gao, Zirui Wu, Xin Jiang, Zhenguo Li, and Lingpeng Kong. Dream 7B: Diffusion Large Language Models, August 2025. URL <http://arxiv.org/abs/2508.15487>. arXiv:2508.15487 [cs].

Appendix

Table of Contents

A	RAGTruth: Span-Level Results	15
	A.1 Retrieval Augmentation	15
	A.2 CDH Localization Curves	15
B	Ablation Studies	15
	B.1 Correction Precision	15
	B.2 Sensitivity: α , T_r , Span, N -Paths	16
	B.3 Confident-but-Wrong Analysis	16
	B.4 Extended Generation Metrics	17
C	Baseline Comparisons	17
	C.1 Per-Dataset Breakdown	17
	C.2 SelfCheckGPT-DLM Comparison	17
D	Statistical Validation	17
E	Implementation Details	18
	E.1 LLM-as-Judge Prompt	18

A RAGTruth: Span-Level Results

Table 4 provides the full per-subset breakdown behind Figure 4. Span reduction is highest on Data2Text (43.7%), where structured facts produce clear-cut uncertain positions; the highest fraction of improved examples is on QA (75.0%), where single-span corrections have the largest relative impact. Positive Δ FS across all subsets confirms that corrections improve factual precision rather than simply deleting content.

Subset	N	Hall.%	AUROC	Δ FS	Span Red.%
QA	788	18.4	0.612	+0.052	38.4
Summary	500	24.2	0.641	+0.073	41.2
Data2Text	500	66.8	0.663	+0.092	43.7
All	1788	33.1	0.639	+0.072	41.1

Table 4: Span-level correction on RAGTruth (LLaDA-8B). Δ FS: FactScore change (positive = more precise). Span Red.: reduction in hallucinated span mass.

A.1 Retrieval Augmentation

Table 5 isolates the effect of retrieval strategy. OSCAR without retrieval (60.8) already exceeds naive RAG (53.5) by 7.3 points, the primary gain is from targeted remasking, not retrieved evidence. Adding targeted span-level retrieval yields a further +3.4 over OSCAR alone, because evidence is fetched for each uncertain claim rather than the full query.

Configuration	F1 (%)	Δ vs. Unguided
Unguided decoding	51.7	—
Naive RAG	53.5	+1.8
OSCAR (no retrieval)	60.8	+9.1
OSCAR + Naive RAG	62.4	+10.7
OSCAR + Targeted RAG	64.2	+12.5

Table 5: Retrieval comparison (LLaDA-8B, TriviaQA + HotpotQA avg F1).

A.2 CDH Localization Curves

Figure 7 shows that hallucinated positions concentrate in the high-entropy tail: examining only the top 20% of positions by cross-chain entropy captures two-thirds of all true errors, making targeted remasking practical without modifying the remaining 80% of tokens. At $k=10\%$, OSCAR already captures 48.2% (vs. 31.5% TraceDet, 10% random), confirming that the unsupervised signal localizes hallucinations more effectively than trained alternatives.

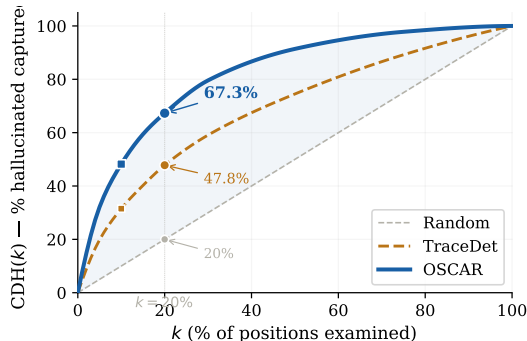


Figure 7: CDH(k) on RAGTruth. At $k=20\%$, OSCAR captures 67.3% of hallucinated positions vs. 47.8% (TraceDet) and 20% (random).

B Ablation Studies

B.1 Correction Precision

Among examples where OSCAR applies a correction, 91.9% are improved on TriviaQA (57 corrected, 5 broken out of 500) and 97.1% on HotpotQA (34 corrected, 1

broken). CommonsenseQA triggers no intervention.

B.2 Sensitivity: α , T_r , Span, N -Paths

α	% Remasked	F1 (%)	AUROC
0.05	5%	64.1	83.8
0.10	10%	66.5	85.1
0.15	15%	68.2	86.0
0.20	19%	69.0	86.5
0.25	25%	68.1	86.3
0.30	30%	66.8	85.9
0.40	40%	63.7	84.2

Table 6: Threshold α sensitivity (LLaDA-8B, QA macro-avg).

Setting	F1 (%) / Δ FS	Cost
<i>Refinement steps T_r</i>		
$T_r=2$	65.4 / +0.041	0.03 \times
$T_r=4$	67.8 / +0.058	0.06 \times
$T_r=8$	69.0 / +0.072	0.10\times
$T_r=16$	69.2 / +0.074	0.19 \times
<i>Span aggregation (w, ℓ_{\min})</i>		
$w=0, \ell=1$	65.8	28.4% red.
$w=1, \ell=3$	67.4	35.2%
$w=2, \ell=3$	69.0	41.1%
$w=3, \ell=3$	68.3	45.8%
$w=2, \ell=5$	67.9	37.6%
<i>N-paths FactScore (RAGTruth)</i>		
$N=1$	Δ FS = -0.030	—
$N=4$	+0.073	—
$N=8$	+0.148	—
$N=16$	+0.048	—

Table 7: Refinement steps T_r , span aggregation, and N -paths FactScore (LLaDA-8B). Defaults bolded.

α plateaus across [0.15, 0.25]; F1 and Δ FS plateau at $T_r=8$; span defaults ($w=2, \ell_{\min}=3$) achieve peak F1; FactScore peaks at $N=8$.

B.3 Confident-but-Wrong Analysis

Dataset	Total Hall.	CBW	Detectable	CBW Rate
TriviaQA	245	38	207	15.5%
HotpotQA	315	63	252	20.0%
RAGTruth	592	53	539	9.0%

Table 8: CBW hallucinations (LLaDA-8B). CBW = $H_{\times,i}=0$ but factually wrong.

80–91% of hallucinated positions expose non-zero cross-chain entropy and are detectable; the remaining CBW cases represent knowledge gaps requiring retrieval rather than remasking.

Dataset	EM		F1		R-L		BLEU	
	Bef.	Aft.	Bef.	Aft.	Bef.	Aft.	Bef.	Aft.
<i>LLaDA-8B</i>								
TriviaQA	51.0	61.4	58.2	68.9±0.3	55.1	65.4	33.2	41.8
HotpotQA	37.0	43.6	45.2	52.7±0.4	42.8	50.1	24.6	30.1
CommQA	85.4	85.4	85.4	85.4±0.0	85.4	85.4	72.1	72.1
<i>Dream-7B</i>								
TriviaQA	42.0	53.8	50.5	61.2±0.5	48.3	58.7	—	—
HotpotQA	30.2	37.4	38.8	46.1±0.6	36.5	43.7	—	—
CommQA	81.2	81.2	81.2	81.2±0.0	81.2	81.2	—	—

Table 9: Full generation metrics before/after OSCAR correction (mean ± std over 3 seeds).

B.4 Extended Generation Metrics

C Baseline Comparisons

C.1 Per-Dataset Breakdown

Method	TrivQA	HotQA	Category
Perplexity	52.1	50.8	Output
LN-Entropy	56.3	53.4	Output
Semantic Entropy	54.7	52.1	Output
Lexical Sim.	61.8	58.7	Output
EigenScore	65.4	61.2	Latent
TSV	58.2	56.8	Latent
OSCAR (EM)	80.3	71.5	Cross-chain
OSCAR (Judge)	89.7	86.7	Cross-chain

Table 10: Fair-baseline AUROC (%) under unified protocol (LLaDA-8B).

All baselines re-evaluated on our DLM outputs under the same pipeline.

C.2 SelfCheckGPT-DLM Comparison

Method	TrivQA	HotQA	Avg
SelfCheck (overlap)	59.3	56.1	57.7
SelfCheck (entropy)	54.8	52.4	53.6
OSCAR (EM)	80.3	71.5	76.4
OSCAR (Judge)	89.7	86.7	86.5

Table 11: SelfCheckGPT-DLM vs. OSCAR (LLaDA-8B, N=8).

OSCAR outperforms the best SelfCheckGPT variant by 18.7 AUROC points; reveal-order diversification exposes a qualitatively different signal than independent resampling.

D Statistical Validation

All Judge CIs on TriviaQA and HotpotQA exclude DynHD’s LLM-as-judge score (84.2).

Dataset	AUROC	95% CI Low	High
TriviaQA (Judge)	89.7	86.8	92.3
HotpotQA (Judge)	86.7	83.2	89.9
CommQA (Judge)	83.4	80.1	86.5
Average (EM)	76.4	73.8	79.1

Table 12: Bootstrap 95% CIs (1,000 resamples, LLaDA-8B).

E Implementation Details

LLM-as-Judge prompt. Applied uniformly to all methods via GPT-4o:

You are evaluating whether an AI-generated answer is factually correct. The answer does not need to match the reference exactly---it should be semantically equivalent and contain the key facts. Rate as CORRECT if the core factual content matches, INCORRECT if it contains factual errors, PARTIAL if partially correct. Respond with only the label.